Thermodynamics and Kinetics of the Reaction of a Single-Chain Antibody Fragment (scFv) with the Leucine Zipper Domain of Transcription Factor GCN4[†]

Susanne Weber-Bornhauser, Jolanda Eggenberger, Ilian Jelesarov, André Bernard, Christine Berger, and Hans Rudolf Bosshard*

Biochemisches Institut der Universität Zürich, Winterthurerstrasse 190, CH-8057 Zürich, Switzerland

Received April 17, 1998; Revised Manuscript Received July 14, 1998

ABSTRACT: Single-chain Fv (scFv) fragments of antibodies have become important analytical and therapeutic tools in biology and medicine. The reaction of scFv fragments has not been well-characterized with respect to the energetics and kinetics of antigen binding. This paper describes the thermodynamic and kinetic behavior of the high-affinity scFv fragment SW1 directed against the dimeric leucine zipper domain of the yeast transcription factor GCN4. The scFv fragment was selected by the phage display technique from the immune repertoire of a mouse that had been immunized with the leucine zipper domain of GCN4. The scFv fragment was produced in high yield in *Escherichia coli* inclusion bodies and refolded from the denatured state. Differential scanning calorimetry showed that SW1 was stable up to about 50 °C, but the subsequent thermal denaturation was irreversible (T_m approximately 68 °C). The scFv fragment specifically recognized the dimeric leucine zipper conformation. Two scFv fragments bound to the GCN4 dimer to form the complex $(scFv)_2$−GCN4. Because of its repetitive structure, the rod-shaped GCN4 leucine zipper may present two similar epitopes for the scFv fragment. Surprisingly, the binding reaction was highly cooperative, that is, the species $(scFv)_2$−GCN4 dominated over scFv−GCN4 even in the presence of a large excess of the antigen GCN4. It is speculated that cooperativity resulted from direct interaction between the two GCN4-bound scFv fragments. At 25 °C, the average binding enthalpy for a scFv fragment was favorable (−61 kJ mol^{-1}), the entropy change was unfavorable, and the change in heat capacity was -1.27 ± 0.14 kJ mol^{-1} K^{-1}. As a result of enthalpy−entropy compensation, the free binding energy was virtually independent of temperature in the physiological temperature range. Antigen binding in solution could be described by a single-exponential reaction with an apparent rate constant of 1×10^6 M^{-1} s^{-1}. Binding followed in a biosensor with the dimeric GCN4 coupled to the surface of the metal oxide sensor chip was 20 times slower.

Antibodies are a diverse yet well-characterized family of proteins (*1*). Due to their very specific recognition of the binding partner, antibodies are widely used in biology and medicine as diagnostic and therapeutic agents (*2*). However, the relatively large size of a whole antibody molecule can impede its practical application. For example, whole antibodies show poor tumor penetration (*3*) and are slowly cleared from the blood circulation (*4*). Furthermore, the immunogenicity of intact immunoglobulins strongly limits the therapeutic use of rodent monoclonal antibodies in humans (*5*).

The finding that the variable domains of an antibody can be functionally expressed in *Escherichia coli* as an Fab (*6*), an Fv (*7*), or an scFv[1] fragment (*8*, *9*) has revolutionized the field of antibody technology. In an scFv fragment, the heavy- and light-chain variable domains are covalently connected through a flexible peptide linker to form the smallest portion of an immunoglobulin that fully retains the binding properties of the whole antibody (*10*). The antigen-binding moiety is made easily accessible to genetic engineering and, in principle, to economical production in bacteria. Antibody fragments against a broad variety of antigens have been isolated by the cloning of antibody repertoires into a combinatorial library followed by selection procedures such as phage display. Affinity and specificity of scFv fragments can be improved by selective mutation (*11*) or by mimicking affinity maturation (*12*). scFv fragments have also been tailored for in vivo applications, for example by fusion of a tumor-targeted scFv fragment with a toxin and intracellular expression (*13*, *14*).

While a lot of work has been dedicated to the design, production, and specificity of scFv fragments, little is known about the thermodynamics and kinetics of the formation of scFv−antigen complexes. The goal of the present work was to gain such information for a scFv fragment directed against the dimeric leucine zipper domain of the basic leucine zipper (bZIP) transcription factor GCN4 from yeast (*15*, *16*). The

[†] This work was supported in part by the Swiss National Science Foundation (Grant No. 3.45556.95)

[1] Abbreviations: bZIP, basic leucine zipper; cfu, colony forming units; DSC, differential scanning calorimetry; DTT, dithiothreitol; EDTA, ethylenediaminetetraacetic acid; ELISA, enzyme-linked immunosorbent assay; GCN4, gene control of amino acid synthesis nonderepressible mutant 4; GdmCl, guanidinium hydrochloride; GSH/GSSG, reduced and oxidized glutathion; HPLC, high-performance liquid chromatography; HRP, horseradish peroxidase; IPTG, isopropylthiogalactoside; ITC, isothermal titration calorimetry; PBS, phosphate-buffered saline; PEG, poly(ethylene glycol); scFv, single-chain Fv; V_H, heavy-chain variable domain; V_L, light-chain variable domain; YT, yeast tryptone.

S0006-2960(98)00874-5 CCC: $15.00
Published on Web 08/26/1998

Table 1: Sequences of GCN4-Derived Peptides Used in this Study[a]

abbreviation	R_1	R_2	X_1	X_2	major conformation
GCN4	N^{α}-acetyl	amide	Asp	Ser	noncovalent coiled coil dimer
$GCN4_{SS}$	N^{α}-acetyl-CGGG	amide	Asp	Ser	disulfide-linked coiled coil dimer
biotin−GCN4	biotin−GGG[b]	amide	Asp	Ser	noncovalent coiled coil dimer
biotin−$GCN4_{SS}$	biotin−GGGCGGG[b]	amide	Asp	Ser	disulfide-linked coiled coil dimer
GCN4(7P14P)	N^{α}-acetyl	amide	Pro	Pro	random coil monomer
$GCN4(7P14P)_{SS}$	N^{α}-acetyl-CGGG	amide	Pro	Pro	disulfide-linked random coil dimer
biotin−GCN4(7P14P)	biotin−GGG[a]	amide	Pro	Pro	random coil monomer
C62GCN4[c]	br[c]	free acid	Asp	Ser	noncovalent coiled coil dimer[d]
$C62GCN4_{SS}$[c]	br[c]	GSGC	Asp	Ser	disulfide-linked coiled coil dimer[d]

[a] R_1-RMKQLEX_1KVEELLX_2KNYHLENEVARLKKLVGER-R_2. [b] Biotin is amide-linked to the N^{α}-amino group. [c] Sixty-two C-terminal residues of GCN4 containing the DNA-binding basic region (br) preceding the leucine zipper domain; br = MIVPESSDPAALKRARNTEAARRSRARKLQR. [d] The br domain of C62GCN4 is unordered when not bound to DNA (*56*).

281-residue GCN4 is composed of a long N-terminal part involved in transcriptional regulation, a short basic region that binds to the major groove of the double-stranded DNA target site, and a C-terminal leucine zipper following immediately after the basic DNA-binding region. The C-terminal ~60 residues comprising the DNA binding region and the leucine zipper suffice to recognize the AP-1 or CRE target DNA sequences (*17*−*19*). We have used a derivative of the 33-residue leucine zipper domain to produce the high-affinity scFv fragment SW1 by repertoire cloning and phage display. Binding of this scFv fragment was analyzed with the leucine zipper domain alone as well as with the C-terminal 62 residues (C62GCN4) encompassing the basic DNA-binding region and leucine zipper domains.

MATERIALS AND METHODS

Antigen Synthesis and Expression of C62GCN4. Synthetic peptides corresponding to C-terminal fragments of GCN4 (Table 1) and the disulfide-linked dimeric leucine zipper LZ_{SS} (sequence Ac-CGGGEYEALEKKLAALEAKLQALEKK-LEALEHG-amide) were synthesized on an Applied Biosystems synthesizer model 430A, using the Rink amide MBHA resin from Novabiochem or the Rapid Amide resin from DuPont, the 9-fluorenylmethyloxycarbonyl (N^{α}-Fmoc) protection strategy, and carboxyl group activation by *O*-benzotriazol-1-yl-*N*,*N*,*N*′,*N*′-tetramethyluroniumhexafluorophosphate/*N*,*N*-diisopropylethylamine (HBTU). The three consecutive terminal glycines were added as Fmoc-$(Gly)_3$ and cysteine as S-(*tert*-butylthio)cysteine. The N^{α}-acetyl group and the N-terminal biotin label were introduced as described (*20*). Cleavage of the peptides from the resin, deprotection, purification by gel filtration, and reversed-phase HPLC were performed as before (*21*). The *S*-*tert*-butylthio group was removed with a 100-fold molar excess of DTT in water overnight at room temperature. The deprotected peptide was purified by reversed-phase HPLC and lyophilized. After dissolving the peptide in 100 mM ammonium hydrogencarbonate, the disulfide bridge was formed overnight at room temperature by air oxidation. The product was again purified on reversed-phase HPLC. C62GCN4 and $C62GCN4_{SS}$ were expressed in *E. coli* (*22*, *23*). The identity of the peptides was confirmed by ion spray mass spectrometry. Peptide concentrations were determined from the absorption at 280 nm measured with the peptides dissolved in 6 M GdmCl, $\epsilon_{280} = 1280\ M^{-1}\ cm^{-1}$ (*24*). Concentrations refer either to a single peptide chain or to the GCN4 dimer, as indicated. For example, 1 μM GCN4 peptide was equivalent to 0.5 μM GCN4 dimer. Disulfide-linked peptides were counted as two peptide chains.

Production of Anti-GCN4 scFv Fragments. A Balb c-mouse was immunized with biotin−$GCN4_{SS}$ coupled to avidin (for the preparation of the immunogen complex and the immunization strategy, see ref *20*). mRNA was extracted from the mouse spleen (QuickPrep mRNA purification kit, Pharmacia Biotech) and transcribed into cDNA using pd-$(N)_6$ primers (first strand cDNA synthesis kit, Pharmacia Biotech). Amplification of V_L and V_H domains, assembly into a single-chain format, cloning into the phage display vector pAK100, and library production were performed as in previous work (*25*). To rescue scFv displaying phages, 50 mL of 2xYT medium containing 1% glucose and 25 μg/mL chloramphenicol was inoculated with approximately 10^9 cells from the glycerol library stock, grown to $OD_{600} = 0.5$ and infected with 10^{12} cfu VCS helper phage (Stratagene). After 10 min at 37 °C, IPTG was added to a 0.5 mM final concentration and the culture was diluted with 150 mL of 2xYT, 25 μg/mL chloramphenicol, and 0.5 mM IPTG. The culture was shaken overnight at 30 °C for phage production. Two hours after infection, 50 μg/mL kanamycin was added. Phage particles were purified and 80-fold concentrated by two subsequent PEG/NaCl precipitations. For selection of GCN4-binding scFv fragments, three rounds of panning were performed. In the first round, selection was by panning on $GCN4_{SS}$ immobilized either on immunotubes (Nunc, Maxisorp) or on magnetic beads (Boehringer Mannheim). For the second and third rounds, 100 μL of antigen-coated magnetic beads was used. For panning on immobilized $GCN4_{SS}$, four immunotubes were coated overnight at 4 °C with 30 μg/mL biotin−$GCN4_{SS}$−streptavidin complex in 35 mM $NaHCO_3$, 15 mM Na_2CO_3, and 0.02% NaN_3, pH 9.6. Tubes were blocked with 5% dried skimmed milk in PBS (8.3 mM Na_2HPO_4, 1.47 mM KH_2PO_4, 137 mM NaCl, 2.7 mM KCl, pH 7.2) for 2 h at room temperature before 0.5 mL of phage (approximately 10^{12} phage particles) in 3 mL of 2.5% dried skimmed milk in PBS was added to each tube and incubated at room temperature for 2 h. Unbound phages were washed off and bound phages in each tube were eluted with one of the following: (a) *E. coli* XL-1 Blue (Stratagene) $OD_{600} = 0.5$, 4 × 3 mL for 5 min each; (b) 0.1 M glycine−HCl pH 2.5; (c) 100 mM triethylamine; or (d) 0.5 mM $GCN4_{SS}$ in PBS. Where appropriate the eluate was neutralized. Each eluate was then added to 20 mL of XL-Blue cells ($OD_{600} = 0.4-0.6$). These sublibraries were plated on 2xYT, 25 μg/mL chloramphenicol, and 1% glucose and

incubated overnight at 37 °C. The colonies were scraped off into 2xYT, combined, and stored in 10% glycerol at −80 °C. Panning on magnetic beads and subsequent infection of XL-Blue cells was done as described (*26*). Concentrations of biotin−$GCN4_{SS}$ were 50 nM in the first and second round and 10 nM in the third round.

Phage ELISA. Single colonies were grown in 2 μL of 2xYT, 25 μg/mL chloramphenicol to an OD_{600} of 0.4−0.7 at 37 °C. Then, 1 mL of 2xYT, 25 μg/mL chloramphenicol, 1.5 mM IPTG, and 10^{10} cfu VCS helper phage was added, and the cultures were incubated overnight at 30 °C. Phage from 1.6 mL of culture supernatant was purified and concentrated 8-fold by PEG−NaCl precipitation. One-hundred microliters of each phage colony was diluted 1:1 with 5% dried skimmed milk in PBS and added to the wells of a microtiter plate (Nunclon MicroWell, Nunc) coated with 10 μg/mL biotin−$GCN4_{SS}$−streptavidin conjugate and blocked with 5% dried skimmed milk in PBS. After 1.5 h of shaking at room temperature, 50 μL of HRP−anti-M13-conjugate (Pharmacia, diluted 1:2000 in 2.5% dried skimmed milk in PBS) was added and incubated for 1 h at room temperature. For detection, 100 μL of soluble BM blue HRP substrate (Boehringer Mannheim) was used. To confirm the specificity of the signal, the phage solution was preincubated for 10 min with 8 μM $GCN4_{SS}$ before it was added to the antigen-coated ELISA wells. Binding clones were sequenced by cycle sequencing (Sequi Therm Long Read Cycle Sequencing Kit LC, Epicenter Technologies) with fluorescent primers and analyzed on a LI-COR DNA sequencer (MWG Biotech).

Expression of Anti-GCN4 scFv Fragment SW1. Clone SW1, which exhibited particularly strong anti-GCN4 activity, was chosen for protein expression in *E. coli*. The corresponding DNA was subcloned into the T7-expression vector pTFT74 (*27*) and transformed into *E. coli* BL21DE3. scFv fragment SW1 was expressed and refolded essentially as described (*28*). An overnight culture in 2xYT, 100 μg/mL ampicillin was diluted 1:40 into 1 L of 2xYT, 100 μg/mL ampicillin and grown at 37 °C. After 4 h, expression was induced with 1 mM IPTG and the culture shaken for another 4 h. Cells were harvested by centrifugation, redissolved in 35 mL of 10 mM Tris−HCl, 2 mM $MgCl_2$, pH 8, and disrupted by sonification. Two micrograms of DNAse, 10 mL of Triton X-100, and EDTA (final concentration of 10 mM) were added, and the inclusion bodies were harvested by centrifugation. The inclusion bodies were washed with 0.1 M Tris−HCl, 0.5 M GdmCl, 10 mM EDTA, pH 8, and then with 100 mM Tris−HCl, 1% Triton X-100, 10 mM EDTA, pH 8. The inclusion body pellet was solubilized in 25 mL of solubilization buffer (200 mM Tris−HCl, 6 M GdmCl, 10 mM EDTA, 20 mM DTT, pH 8). After a short centrifugation at 20000*g*, the supernatant was dialyzed against solubilization buffer without DTT, then diluted 100-fold into refolding buffer (0.5 mM ε-amino-*N*-caproic acid, 0.5 mM benzamidinium−HCl, 1 mM oxidized glutathione, 0.2 mM reduced glutathione, 0.8 M arginine, 0.2 M Tris−HCl, 2 mM EDTA, pH 9) and incubated 24−48 h at 4 °C. The pH of the refolding solution was adjusted to 7.5 with concentrated HCl before biotin−$GCN4_{SS}$ coupled to immobilized streptavidin (Pierce ImmunoPure) was added and the antigen-scFv complex was allowed to form overnight at 4 °C. The solution was filtered and the affinity material with the bound scFv fragment poured into a column. After washing with 0.25×PBS, the scFv fragment was eluted with 100 mM glycine−HCl, pH 2.8, and the eluate immediately neutralized with 2 M Tris and dialyzed against PBS. The identity of the antibody fragment was checked by ion spray mass spectrometry: 27 464.6 (calculated), 27 464.9 (found). The protein concentration was determined by absorption measurement under denaturing conditions using ϵ_{280} = 49 170 M^{-1} cm^{-1} (*24*). The protein was stored at 4 or −20 °C.

Competition ELISA. For this assay scFv fragment SW1 was expressed with a C-terminal histidine tag (His_5) in the pTFT74 vector and purified as described above. A Nunclon MicroWell plate was coated with 10 μg/mL streptavidin−biotin−$GCN4_{SS}$ conjugate. After washing with PBS−0.02% Tween, the plate was blocked with 5% dried skimmed milk in PBS. Competitor antigens to be tested for cross-reactivity were diluted serially in a separate PetraPlastic plate in 2% dried skimmed milk in PBS. To each dilution, a solution of scFv fragment SW1 was added to a final concentration of 9.6×10^{-8} M and the mixture incubated for 1 h. The scFv solution preincubated with the competitor antigen was then added to the $GCN4_{SS}$-coated, blocked, and washed Nunclon plate. After incubation for 1 h at room temperature, bound scFv fragment was detected by anti-His-tag monoclonal antibody 3D5 (*29*) and an anti-mouse IgG peroxidase conjugate (Pharmacia) using soluble BM blue HRP substrate.

Gel Chromatography. The SMART system from Pharmacia Biotech was used. Typically, 50 μL of a protein solution in PBS was loaded onto a Superdex 75 column. The protein was eluted at 25 °C with PBS, the flow rate was 60 μL/min, and the eluate was monitored at 280 nm.

Fluorescence Titration. A Spex Fluorolog spectrofluorimeter was used. The temperature was held constant at 11, 18, 25, or 30 °C, and the spectra were taken in 0.5-nm steps with an integration time of 1 s. Typically, 180 nM scFv fragment in 3 mL of PBS was placed in the cuvette and titrated with 5 μM $C62GCN4_{SS}$ dimer added in 5−10-μL aliquots. After each addition the solution was stirred for 5 min before the emission spectrum from 300 to 400 nm (excitation 280 nm) was measured. The buffer spectrum was subtracted, and the fluorescence was integrated from 324 to 347 nm and normalized to calculate the fractional degree of saturation $Y = \Delta F/\Delta F_{max}$. Titration curves were fitted by the following:

$$Y = \{D_0 + P_0 + 1/K - [(D_0 + P_0 + 1/K)^2 - 4D_0P_0]^{1/2}\}/2D_0 \quad (1)$$

where D_0 is the concentration of the scFv fragment and P_0 that of the GCN4 peptide chains, that is, the concentration of dimeric GCN4 was $P_0/2$. D_0 and K were the fitting parameters.

Isothermal Titration Calorimetry. ITC experiments were performed using an OMEGA titration calorimeter (Microcal Inc., Northampton, MA) (*30*). Measurements were done as described in detail before (*31*). Thoroughly degassed scFv solution (5−10 μM) was placed in the cell. The injection syringe was filled with 130−200 μM antigen solution. The same batch of buffer was used for the antigen and the scFv fragment to minimize artifacts due to minor differences in buffer composition. The rotation speed of the syringe was

300 rpm. After equilibration to baseline stability, the titration experiment consisted of 15 injections, each of 8-μL volume and 10-s duration, with an interval between injections of 300 s. The titration data were corrected for the small heat changes observed for injections after saturation and analyzed with the software provided with the instrument (*30*). The total heat of binding, ΔH, was obtained by nonlinear least-squares fitting of the data to a 1:1 or 2:1 binding model, as implemented in the data analysis software of the instrument.

Differential Scanning Calorimetry. Experiments were performed with the VP microcalorimeter (MicroCal Inc., Northampton) at a scan rate of 1 deg min^{-1}. Technical details and performance of the instrument have been described recently (*32*). Protein samples were thoroughly dialyzed and degassed prior to the measurement. The protein concentration was 20 μM in PBS or in 10 mM sodium acetate buffer, pH 5.5.

Stopped-Flow Measurements. Binding kinetics were measured on a SF-61 stopped-flow spectrofluorimeter (High Tech Scientific Ltd., Salisbury, U.K.) as described (*33*). Equal volumes of scFv fragment and antigen solutions were mixed, and the emission of the intrinsic tryptophan fluorescence was measured (excitation 295 nm, emission above 320 nm). The temperature was held at 11 °C. The final antigen concentration was at least 8 times above the scFv fragment concentration, which was 0.5 μM.

Biosensor Measurements. The grating coupler sensor BIOS-1 from Artificial Sensing Instruments, Zürich, Switzerland, was used to determine the binding kinetics between the scFv fragment SW1 in solution and biotin−$GCN4_{SS}$ coupled to the biosensor surface through avidin. The light source was a HeNe laser of 632.8 nm (*34*). SiO_2−TiO_2 or Ta_2O_5 sensor chips (ASI 1400 or ASI 3200, obtained from Artificial Sensing Instruments, Zürich) were used as substrates for ligand immobilization. A silicon cuvette (10-μL volume) connected via Teflon tubings to a peristaltic pump provided the flow-through cell. The flow rate was set at 10 μL/min for immobilization chemistry and at 70 μL/min for kinetic measurements. Sensor chips were cleaned by sonification in ethanol−water (1:2) for 5 min, rinsed with ethanol, and dried under a stream of nitrogen. The cleaned chips were rendered hydrophilic in an oxygen plasma (Technics Plasma, Florence, KY) for 20 s at a load coil power of 200 W and an oxygen pressure of 0.8 Torr. The hydrophilic sensor chips were immediately transferred to the silanization solution composed of 10% (aminopropyl)triethoxysilane (Fluka) in water, pH 6, adjusted with acetic acid, and heated to 80 °C for 2 h under reflux. After being rinsed copiously with water and immersed in PBS, the silanized chips were ready for chemical modification with NeutrAvidin (Pierce). To this end, the freshly silanized sensor chips were mounted in the flow-through cell of the instrument and flushed with PBS to establish a stable baseline. Covalent immobilization of NeutrAvidin was accomplished by activation of the chip with 5 mM of the bivalent cross-linker bis(sulfosuccinimidyl)suberate (Pierce) in 10 mM acetate buffer, pH 5.0, for 10 min followed by reaction with NeutrAvidin (100 μg/mL in acetate buffer, pH 5.0) for 40 min. Thereafter, the chip was rinsed with 10 mM HCl to clear nonreacted material. Following this protocol a dense layer of NeutrAvidin at a surface coverage of 5.1 ng/mm^2 was obtained. The surface density was calculated from the transverse electric and the transverse magnetic components of the in-coupled laser beam (*34*). The chips thus modified served to bind biotin−$GCN4_{SS}$. Biotin−$GCN4_{SS}$ (120 nM) was pumped over the chip for 1 min after which time the coupling density of avidin-bound biotin−$GCN4_{SS}$ was 1.2 ng/mm^2. The chips were then used to measure the rates of binding and dissociation of the scFv fragment SW1, which was pumped over the surface of the chip at a series of different concentrations. Data analysis was performed using nonlinear least-squares fitting routines programmed in Origin (Microcal).

RESULTS

Production and Expression of the scFv Fragment SW1. A mouse was immunized with the disulfide-linked peptide biotin−$GCN4_{SS}$ (Table 1) coupled to avidin as a carrier (*20*). In biotin−$GCN4_{SS}$ the biotin group was separated from the disulfide bridge by a triglycine spacer to facilitate the access of the biotin group to the binding cavity of avidin. Another triglycine spacer separated the disulfide bridge from the leucine zipper. A cDNA library was constructed using mRNA isolated from spleen cells of the immunized mouse. V_H and V_L domains of the immunoglobulins present in this library were selectively amplified by PCR and assembled into the scFv format in the orientation V_L-linker-V_H (*25*). The peptide linker between the C-terminus of V_L and the N-terminus of V_H had the sequence $(Gly_4Ser)_4$. scFv molecules with a 20-residue linker are predominantly monomeric while shorter linkers tend to produce dimeric and oligomeric scFv fragments (*35*). The scFv library was cloned into the phage display vector pAK100 (*25*), and scFv displaying phages were produced. The panning procedure was done such that in the first round the diversity of binders selected was as broad as possible. This was achieved by different modes of eluting the phage from plastic-bound antigen and, in parallel, by selection on antigen-coated magnetic beads. In panning rounds two and three, only the magnetic beads in solution were used, after which 50% of the clones tested showed binding to the antigen in the phage ELISA. Their interaction with biotin−$GCN4_{SS}$ could be completely inhibited by 8×10^{-6} M soluble $GCN4_{SS}$, demonstrating the desired specificity.

Clone SW1 was selected for protein expression in *E. coli*. SW1 was cloned in the pTFT74 vector under the control of a T7 promotor, and the scFv fragment was produced as cytoplasmic inclusion bodies in *E. coli* following induction with IPTG. Inclusion bodies were isolated, partially purified, and solubilized under denaturing and reducing conditions. After dialysis against denaturing buffer without DTT, the scFv fragment was refolded by 1:100 dilution into refolding buffer containing the redox-shuffling system GSH/GSSG. Pure scFv fragment was produced in a single step by affinity-purification on immobilized $GCN4_{SS}$ (Figure 1). The yield was approximately three milligrams of functional scFv fragment per liter of culture and per OD_{600}. The calculated molecular mass of 27.5 kDa was confirmed by mass spectrometry. The nucleotide sequences have been deposited in the EMBL Nucleotide Sequence Database under the accession numbers Y16621 (V_H chain) and Y16622 (V_L chain).

Antigen Specificity. The specificity was tested in a competition ELISA. Binding of the scFv fragment to

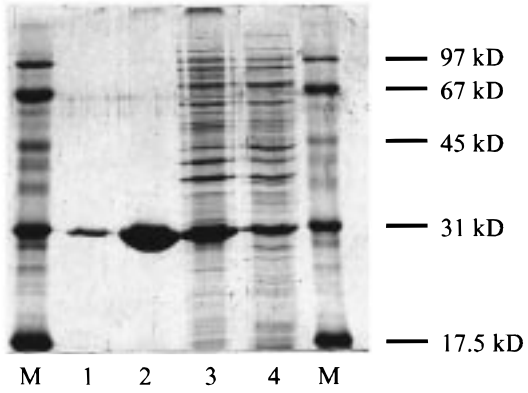

FIGURE 1: SDS−polyacrylamide gel electrophoresis of expression products. Proteins from bacterial inclusion bodies were run on a reducing 12.5% gel and stained with Coomassie-blue: lanes 1 and 2, 35 and 350 pmol of affinity-purified scFv fragment; lane 3, whole inclusion bodies; lane 4, total bacterial protein after induction; M, molecular mass markers.

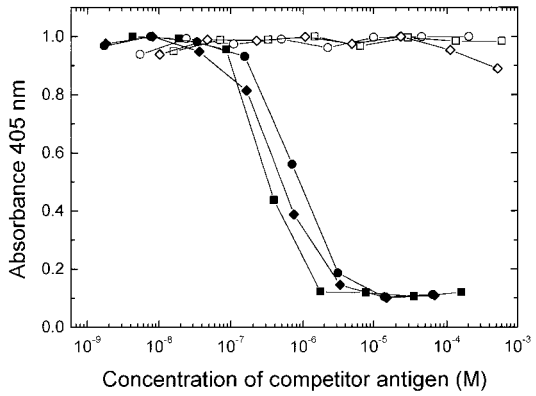

FIGURE 2: Antigen specificity of the scFv fragment SW1 determined by competition ELISA. The scFv fragment was preincubated with increasing amounts of competitor antigen before reaction with $GCN4_{SS}$ coated to the ELISA plate through biotin−streptavidin. Bound scFv fragment was detected with anti-His-tag antibody followed by an anti-mouse IgG peroxidase conjugate. Competitor antigens: $GCN4_{SS}$ (■), C62GCN4 (◆), $C62GCN4_{SS}$ (●), GCN4-(7P14P) (□), $GCN4(7P14P)_{SS}$ (○), and unrelated disulfide-linked leucine zipper LZ_{SS} (◇).

$GCN4_{SS}$ bound to the ELISA plate through biotin−streptavidin was challenged by preincubation of the scFv fragment with different peptides. The results are shown in Figure 2. Only peptides that contained the sequence of the leucine zipper domain of GCN4 and that were predominantly in the dimeric coiled coil conformation (Table 1) competed with binding to plate-bound $GCN4_{SS}$ (filled symbols in Figure 2). The longer peptides C62GCN4 and $C62GCN4_{SS}$, which contain the basic DNA-binding region preceding the leucine zipper domain, were equivalent competitors. The unrelated dimeric leucine zipper LZ_{SS} (*21*) whose sequence differs significantly from that of $GCN4_{SS}$ was not recognized by SW1.

Dimeric C62GCN4 binds the palindromic AP-1 or CRE site through the basic region peptide. In the crystal, the basic region contacts the major groove of the DNA and the leucine zipper domain is perpendicular to the axis of the DNA (*36, 37*). Therefore, the scFv fragment SW1 should not interfere with DNA binding if its epitope is on the leucine zipper. A complex composed of C62GCN4 and the 20-base-pair oligonucleotide TTCCT**ATGACTCAT**CCAGTT (AP-1 site in bold) (*22*) was prepared. This protein−DNA complex inhibited binding to $GCN4_{SS}$ to the same extent as C62GCN4 alone. That is, the competition curves for C62GCN4 in the presence and in the absence of the 20-base-pair oligonucleotide overlapped completely indicating that the scFv fragment did not interfere with DNA binding to the transcription factor (not shown).

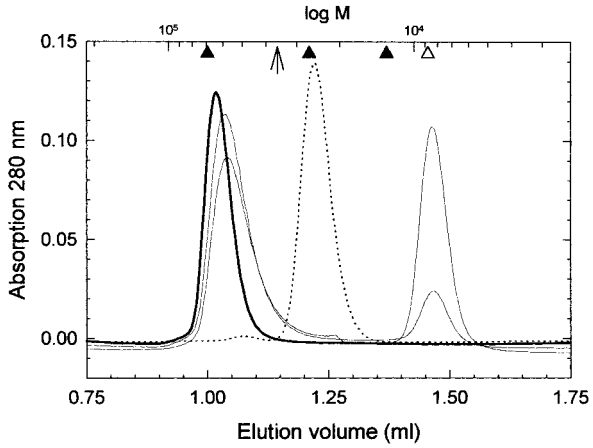

FIGURE 3: Gel chromatography of scFv fragment SW1 alone and bound to GCN4 dimer. Protein (50 μL) was chromatographed on a column of Superdex G75 at 25 °C in PBS. Thick line: 5.5 μM each of scFv and GCN4 peptide. Thin lines: 5.5 μM scFv and 55 μM or 182 μM GCN4 peptide corresponding to, respectively, a 5-fold and 16.5-fold excess of GCN4 dimer over scFv. Dotted line: 5.5 μM scFv. Open triangle: Elution position of dimeric GCN4 (8.8 kDa). Filled triangle: Elution position of BSA (67 kDa), carbonic anhydrase (29 kDa), and cytochrome *c* (12.5 kDa), respectively. Arrow: Expected elution position of a complex with one scFv per GCN4 dimer.

To test whether SW1 was specific for the coiled coil conformation, the random coil derivatives GCN4(7P14P) and $GCN4(7P14P)_{SS}$ were tested. These peptides contain two helix-breaking proline substitutions that induce a random coil structure (*20*). No reaction was seen with the proline-containing derivatives (Figure 2).

Aggregation State of scFv. scFv fragments tend to form dimers and oligomers depending on their sequence and on the length of the linker between V_L and V_H (*35, 38, 39*). In gel chromatography, the scFv fragment moved as a single symmetrical peak of apparent molecular mass 24 kDa, below the calculated mass[2] of 29.5 kDa (dotted line in Figure 3). The reason for the lower than expected apparent mass is unknown. A very small peak with apparent mass 48 kDa was seen in some chromatograms indicating a trace of dimeric scFv fragment. However, free scFv fragment was essentially monomeric under the conditions of the gel chromatography experiment (Figure 3).

Binding Stoichiometry from Gel Chromatography. To determine the stoichiometry of the scFv−antigen complex, the gel chromatography experiments shown in Figure 3 were performed. A sample composed of 5.5 μM scFv fragment SW1 and 5.5 μM peptide chain (equivalent to 2 scFv fragments/GCN4 dimer) eluted as a single peak with an apparent mass of 64 kDa. No free GCN4 was detected. The mass of 64 kDa corresponded to the complex $(scFv)_2$−GCN4, that is, to two scFv fragments bound per one GCN4 dimer. There had to be two epitopes for the scFv fragment

[2] The scFv with a His tag was used in this experiment, hence the mass of 29.5 kDa.

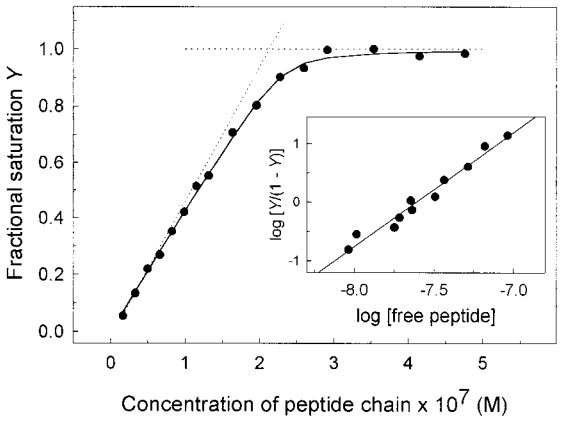

FIGURE 4: Fluorescence titration of the scFv fragment SW1 with antigen. scFv fragment (0.18 μM) was titrated with C62GCN4$_{SS}$ at 11 °C and the fractional saturation $Y = \Delta F/\Delta F_{max}$ plotted against the total concentration of peptide chains (disulfide-linked C62GCN4$_{SS}$ is considered as 2 peptide chains). The solid line is a best fit according to eq 1 for $K = 1.5 \times 10^8$ M^{-1} and [scFv] = 0.2 μM. The crossover point of the dotted lines indicates a stoichiometry of one scFv fragment per peptide chain. Inset: Hill plot of titration data according to $\log\{(Y/(1 - Y)\} = \log K_{Hill} + n_H \log$[free peptide chain], where [free peptide chain] = [peptide]$_{tot} - Y$[scFv]$_{tot}$. The solid line is a best fit for $n_H = 1.94$ and $\log K_{Hill} = 2 \times 10^{15}$. Data points for Y <0.2 and >0.9 have been omitted because of very high scatter.

on the dimeric leucine zipper. As a test for a 2:1 stoichiometry, the chromatography was repeated with the GCN4 dimer in 5- and 16.5-fold excess over the scFv fragment, respectively. Under these conditions, scFv−GCN4 should dominate over (scFv)$_2$−GCN4 if the two binding sites on GCN4 are independent. However, no peak was seen at the expected elution volume of 1.16 mL (arrow in Figure 3).[3] Though the peaks became broader when GCN4 was in excess, their elution position was only slightly shifted to the right indicating but a small amount of scFv−GCN4 in equilibrium with (scFv)$_2$−GCN4. Thus, even in the presence of excess GCN4, the 2:1 complex dominated. This pointed to a cooperative binding event.

Fluorescence Titration. Binding to the antigen quenched the intrinsic Trp fluorescence of the scFv fragment. Figure 4 shows a representative titration of 0.18 μM scFv fragment with C62GCN4$_{SS}$ at 25 °C. Disulfide-linked antigen was used in this experiment to prevent dissociation of GCN4 into monomers. The curve was fitted with the help of eq 1 to obtain [scFv] = 0.2 μM, in good agreement with the nominal scFv concentration of 0.18 μM utilized in the experiment. This confirmed a stoichiometry of one scFv fragment per peptide chain (crossover of dotted lines in Figure 4 is at 0.2 μM peptide concentration). The inset of Figure 4 shows the Hill plot of the fluorescence data. The Hill coefficient (slope) was $n_H = 1.94 \pm 0.23$, confirming very strong cooperativity between the two scFv molecules bound to the GCN4 dimer.

The equilibrium constant estimated from the Hill plot was $(3 \pm 2) \times 10^{15}$ M^{-2}. If there is only (scFv)$_2$−GCN4 (maximum cooperativity), K_{Hill} corresponds to the ternary binding constant of the complex. An apparent binding

[3] The elution position was confirmed by chromatography of a complex of the unrelated scFv fragment JH5 with a 30-residue peptide (C. Berger, unpublished).

Table 2: Thermodynamic Parameters for the Binding of scFv Fragment SW1[a]

T (K)	K ($\times 10^{-8}$)[b,c] (M^{-1})	ΔG[b] (kJ mol^{-1})	ΔH[d] (kJ mol^{-1})	$T\Delta S$[e] (kJ mol^{-1})
284	1.5 ± 0.6	-44.5 ± 1.3	-44.8 ± 0.7	-0.3 ± 2.0
291	1.7 ± 1.2	-45.9 ± 3.1	-48.3 ± 0.8	-2.4 ± 3.9
298	0.7 ± 0.4	-44.8 ± 2.4	-60.8 ± 0.9	-16.0 ± 3.3
298[f]	1.3 ± 0.3	-46.3 ± 0.7	nd	nd
303	3.3 ± 2.0	-49.2 ± 2.8	-65.6 ± 1.1	-16.4 ± 3.9

[a] Average values per one scFv fragment bound to dimeric GCN4. [b] From fluorescence titration, fit according to eq 1. [c] Fitting error, eq 1. [d] From ITC. [e] $T\Delta S = \Delta H - \Delta G$. [f] Binding to the C62GCN4−DNA complex.

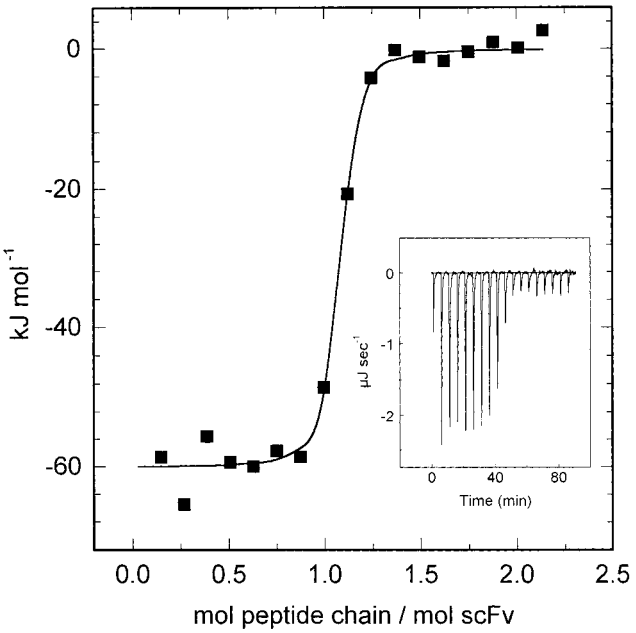

FIGURE 5: Isothermal titration calorimetry of scFv fragment SW1 with C62GCN4 at 25 °C. The solid line is a best fit for $\Delta H = -60.8$ kJ mol^{-1} and a stoichiometry of $n = 1.96$ scFv fragments/GCN4 dimer. Inset: Raw data; the last seven peaks represent the heat released on addition of excess C62GCN4 to the saturated complex. This extra heat is corrected for in the main figure.

constant K for each scFv fragment could be obtained from a fit according to eq 1 of the fluorescence titration shown in the main plot of Figure 4. K was equal to $(1.5 \pm 1.0) \times 10^8$ M^{-1}, which is approximately $\sqrt{K_{Hill}}$ in agreement with high cooperativity.

Fluorescence titrations were also performed with the C62GCN4−DNA complex. The same results were obtained in the presence and in the absence of the AP-1 DNA target (Table 2).

Isothermal Titration Calorimetry. These experiments were performed to determine the thermodynamic parameters of binding and to corroborate the stoichiometry by yet another independent method. Figure 5 shows a representative experiment in which 6.7 μM scFv fragment was titrated with C62GCN4. The data were fit to a 1:1 and a 2:1 binding model, that is for 1 or 2 scFv fragments bound per GCN4 dimer. Good fits were obtained only with the model corresponding to two scFv bound per dimeric GCN4. ΔH was negative and decreased in the range 11−30 °C. Higher temperatures could not be tested since C62GCN4 begins to unfold above 30 °C (*22*). The change of ΔH with temper-

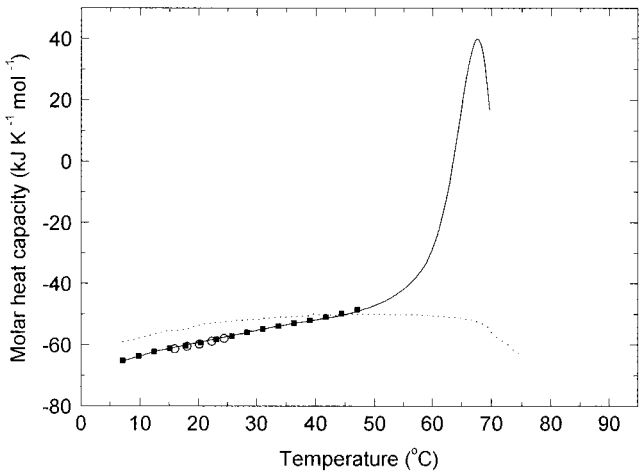

FIGURE 6: Thermal unfolding of the scFv fragment SW1 determined by differential scanning calorimetry. The change of the partial molar heat capacity with temperature of 20 μM scFv fragment in 10 mM sodium acetate, pH 5.5, is shown. The transition peak (solid line) has a maximum at 68 °C but is irreversible on rescanning (dotted line). Open circles and filled squares represent results from prescans between 5 and 50 °C of the same sample. Heating rate 1 K min^{-1}.

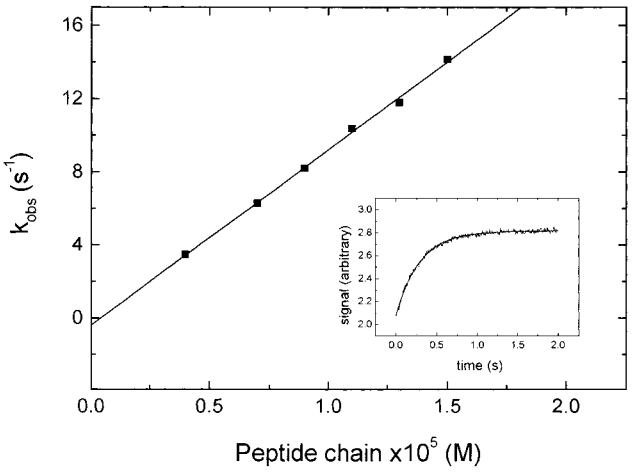

FIGURE 7: Binding kinetics measured by fluorescence stopped flow. The main plot corresponds to eq 2 in the text, which is valid for a pseudo-first-order reaction with $[\text{peptide}]_{tot} \gg [\text{scFv}]$. The negative value of the ordinate intercept is due to the scatter of the experimental data. The true value of k_{off} is, of course, positive but much below 1 (see text). Inset: Trace for the reaction of 0.5 μM scFv fragment with 4 μM C62GCN4 as a representative example. The solid line is a best fit for $k_{obs} = 3.5$ s^{-1}.

ature was linear with a slope of $\Delta C_P = -1.27 \pm 0.14$ kJ mol^{-1} K^{-1}. Because of binding cooperativity, the parameters from ITC are apparent values for each of the two GCN4-bound scFv fragments. The apparent free-energy change was calculated as $\Delta G = -RT\ln K$, where K is the apparent equilibrium constant from fluorescence titration (eq 1). The thermodynamic parameters are listed in Table 2.

To show that the measured ΔH was equivalent to the actual binding enthalpy and was not affected by a change of the protonation state of the scFv fragment or the antigen, the titration was performed in PBS and also in 50 mM Tris−HCl, pH 7.2, with the ionic strength and ion composition adjusted to that of PBS. ΔH was the same in both buffers within error, demonstrating that the formation of the scFv−GCN4 complex was not accompanied by the uptake or release of protons, which would have led to different apparent ΔH values because the two buffers differed in their heat of ionization by 42 kJ mol^{-1} (*40*). Furthermore, association/dissociation of C62GCN4 could have affected the measured heat change. However, as shown before (*22*), the fraction of monomeric C62GCN4 was negligibly small under the conditions of the ITC experiment since the total peptide concentration was always well above the dissociation constant estimated at 10^{-7}−10^{-8} M (*41, 42*).

Thermal Stability of the scFv Fragment. Figure 6 shows a DSC trace. The protein SW1 was stable in the range 2−50 °C. The reversibility of the temperature scan was excellent, and we did not observe any change in the partial molar heat capacity in four repeated scans in this temperature interval. This testifies for good thermal stability and for the monodisperse nature of the scFv fragment SW1 in the physiological temperature range. The apparent thermal unfolding transition was sharp with a midpoint at 68 °C. However, unfolding was irreversible due to aggregation and/or chemical modification at higher temperatures. Thermal scans were identical in PBS (pH 7.2) and sodium acetate (pH 5.5), except that the post-transitional aggregation was significantly more prominent in PBS than in sodium acetate. The partial specific heat capacity of the folded scFv fragment was a linear function of temperature with a slope of $(15 \pm 3) \times 10^{-3}$ J K^{-2} g^{-1}.

Kinetics of Antigen Binding. The change of the intrinsic Trp fluorescence of the scFv fragment was used to follow the kinetics of antigen binding by stopped flow. Figure 7 summarizes the results for C62GCN4 measured at 11 °C. The binding reaction was conducted under pseudo-first-order conditions with the antigen in 8−30-fold excess over the scFv fragment. The kinetic traces were well-described by a single-exponential equation with the apparent rate constants k_{obs} (Figure 7, inset). The plot of k_{obs} against the total antigen concentration was linear in accord with a pseudo-first-order reaction for which k_{obs} is related to the total concentration of the antigen peptide according to

$$k_{obs} = k_{on}[\text{peptide}]_{tot} + k_{off} \qquad (2)$$

The slope of the line in Figure 7 yields $k_{on} = (0.96 \pm 0.02) \times 10^6$ M^{-1} s^{-1}. Because the species $(\text{scFv})_2$−GCN4 was highly populated even under the pseudo-first-order conditions of the stopped-flow experiment, k_{on} is an apparent rate constant for the binding of a scFv to the GCN4 dimer. Although the concentration of scFv−GCN4 was negligible, the 1:1 complex had to be formed on the way to $(\text{scFv})_2$−GCN4 since direct formation of $(\text{scFv})_2$−GCN4 in a ternary reaction was statistically unlikely. However, because of the high cooperativity the 1:1 intermediate was not seen and the overall reaction appeared monophasic.[4] k_{off} was too small to be estimated from the intercept of the plot as the reaction was virtually irreversible. With an apparent K of 1.5×10^8 M^{-1} from fluorescence titration at 11 °C (Table 2), the

[4] Positive cooperativity can be expressed as two consecutive reactions of which the second is faster than the first: $2\text{scFv} + \text{GCN4} \xrightarrow{k_1} \text{scFv:GCN4} + \text{scFv} \xrightarrow{k_2} (\text{scFv})_2\text{:GCN4}$. If the back reactions are slow compared to the on reactions, as was the case, k_{obs} measured by stopped-flow can be approximated by $k_1[\text{GCN4}]$ (*57*).

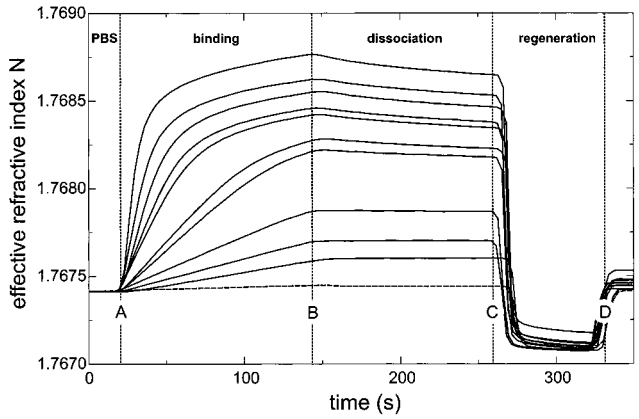

FIGURE 8: Binding kinetics measured in a grating coupler biosensor. An overlay sensorgram for the reaction of scFv fragment SW1 with biotin−$GCN4_{SS}$ immobilized on the sensor surface via NeutrAvidin is shown. The traces correspond to (top to bottom) 2.2, 1.1, 0.8, 0.55, 0.4, 0.275, 0.2, 0.138, 0.1, and 0.069 μM scFv fragment SW1 pumped over the sensor surface in the time interval A−B. Dissociation was started at B by a switch back to pure buffer. The surface was regenerated by a short pulse of 10 mM HCl followed by buffer (interval C−D). The unrelated scFv 4D5 (500 nM, dashed line) served as a control for nonspecific binding, which was negligible.

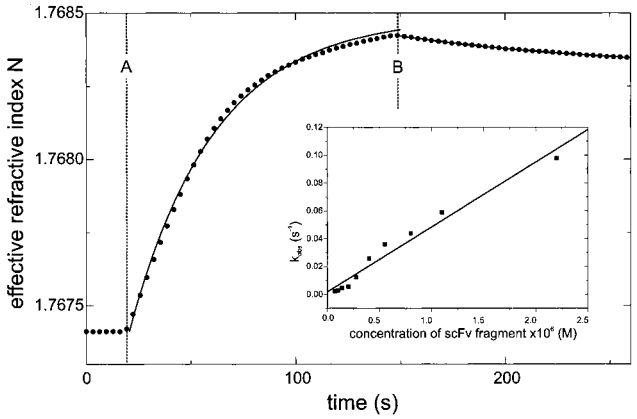

FIGURE 9: Representative kinetic trace observed in the biosensor (0.4 μM scFv). The solid line corresponds to a single-exponential binding reaction and a single-exponential dissociation reaction, respectively. The deviation of the experimental data in the association phase is nonrandom, a sign that the binding reaction at the solid/liquid interfaces is not adequately described by a two-state reaction. Inset: Plot of k_{obs} against the total concentration of the scFv fragment in the buffer flow. Slope and intercept of this plot yield $k_{on} = (4.7 \pm 0.3) \times 10^4$ M^{-1} s^{-1} and $k_{off} \approx 2 \times 10^{-3}$ s^{-1}.

apparent k_{off} was 6.0×10^{-3} s^{-1}, equivalent to a half-time of dissociation of 2 min.

The stopped-flow experiments were repeated in the presence of saturating concentrations of the 20-base-pair nucleotide with the AP-1 target sequence (*22*). Binding rates were independent of DNA (not shown).

Biosensor Studies. A grating coupler sensor was used to measure binding of the scFv fragment SW1 to surface-immobilized biotin−$GCN4_{SS}$. The instrument is based on integrated optics and measures the phase shift of a light wave coupled into a waveguide embossed on the sensor surface. The shift is caused by the absorption of an analyte, here the scFv fragment, to a ligand coupled to the waveguide, here the antigen biotin−$GCN4_{SS}$. (See ref *34* for a description of the instrument and ref *43* for a recent review of optical biosensors). A covalently immobilized monolayer of NeutrAvidin on a plane SiO_2−TiO_2 surface (*34*) served to couple the biotinylated antigen and prevented nonspecific binding to the metal oxide surface. The surface density of biotin−$GCN4_{SS}$ was 1.3×10^{-13} mol/mm^2. This high ligand density gave a good signal-to-noise ratio at low concentrations of scFv fragment. However, the high ligand density could have led to mass transport limitation; this means that the observed binding rate could have been governed by the rate of diffusion of the scFv fragment from the bulk liquid to the sensor surface (*44*). To rule out this possibility, the flow was set at 70 μL/min where the signal change was independent of the flow rate and, therefore, reflected the association reaction proper.

A kinetic experiment consisted of three phases. The association phase (A to B in Figure 8) was initiated by pumping a solution of the scFv fragment over the sensor surface previously equilibrated with buffer. Ten different concentrations of scFv, from 69 nM to 2.2 μM, were reacted with the biotin−$GCN4_{SS}$ on the sensor chip. Dissociation (B to C in Figure 8) was started by a switch back to pure buffer. Finally, the sensor chip was regenerated by a short pulse of 10 mM HCl followed by buffer (C to D in Figure 8). The avidin-bound biotin−$GCN4_{SS}$ resisted the acidic regeneration conditions since the kinetic traces were reproducible even after 20 regeneration cycles. Binding was specific as no signal (apart from a bulk refractive index effect) was observed when the scFv fragment SW1 was preincubated with a 10-fold excess of $GCN4_{SS}$ before addition to the sensor surface (not shown). Moreover, no signal was seen with a 500 nM solution of the unrelated scFv fragment 4D5 (bottom trace in Figure 5).

The binding traces were fit by a single-exponential reaction. Such a fit seemed reasonable in view of the results from the stopped-flow experiments with the reactants free in solution. The values of k_{obs} calculated from the binding traces were plotted against the total concentration of the scFv fragment in the solution pumped over the surface of the sensor chip to obtain k_{on}. The plot is shown in the inset of Figure 9. Linearity was only approximate, and the data points were nonrandomly distributed. This is also reflected in the main part of Figure 9 where the residuals of the experimental data points exhibit a nonrandom distribution around the best fit to a single exponential. Thus, a two-state equilibrium did not adequately describe the association reaction between the surface-bound antigen and the scFv fragment in solution. Assuming a two-state equilibrium as a first approximation, the plot in the inset of Figure 9 gives $k_{on} = (4.7 \pm 0.3) \times 10^4$ M^{-1} s^{-1} and $k_{off} \approx 2 \times 10^{-3}$ s^{-1}. Another way to extract k_{obs} from the data in Figure 8 is to plot the first derivative of the signal with time, dN/dt, against the signal N to obtain a line with the slope k_{obs} (*45*). This analysis gave consistent results: $k_{on} = (6.4 \pm 0.3) \times 10^4$ M^{-1} s^{-1} and $k_{off} \approx 10^{-3}$ s^{-1}. Thus, binding of the scFv fragment to the surface-bound GCN4 dimer was 20 times slower than in the reaction free in solution. The rate difference may have been even larger because the biosensor experiment was conducted at 25 °C and the stopped-flow experiment at 11 °C.

Direct determination of k_{off} from the dissociation phase (B−C in Figure 8) gave $k_{off} = (8 \pm 2) \times 10^{-3}$ s^{-1}. The fit of the dissociation phase to a single exponential decay reaction was good, yet dissociation did not reach the baseline

level even after very long flushing with buffer. A substantial fraction of the scFv fragment remained bound to the sensor surface and was removed only on regeneration with dilute HCl.

DISCUSSION

Production and Antigen Specificity of scFv Fragment SW1. The single-chain fragment was obtained from a mouse immune library by phage display selection using antigen-coated magnetic beads. This had the advantage that a defined antigen concentration in the nanomolar range could be employed to search for strong binders. Also, *E. coli* could be directly infected with the washed magnetic beads carrying the antigen−scFv−phage complex. In this way elution of antigen-bound phages for re-infection, a procedure in which tight binders can be lost, was circumvented. The 20-residue spacer linking V_L with V_H produced predominantly monomeric scFv with hardly a trace of dimer visible when micromolar concentrations of scFv were chromatographed on a Sephadex column. Since the mouse from which the immune library was obtained had been immunized with the disulfide-linked GCN4 dimer, one expected the scFv to be directed against the coiled coil conformation. This was confirmed with several monomeric and dimeric derivatives of GCN4 in competition immuno assays.

Stoichiometry of the scFv−GCN4 Complex. Since the scFv fragment was monomeric and specific for the coiled coil dimer, the stoichiometry of two scFv fragments per dimeric coiled coil was unexpected. How can a small molecule like the leucine zipper domain of GCN4 present two epitopes for two identical scFv fragments? In the leucine zipper, two parallel chains form a rope about 4.5 nm long and 1.5 nm in diameter. Because the sequence of the leucine zipper is repetitive, the same or very similar epitopes may be formed twice. Incidentally, two epitopes for a monoclonal antibody were found on another leucine zipper (*20*).

The high cooperativity of the two binding sites is puzzling. In the case of classical cooperativity between two binding sites, binding of the first scFv changes the conformation of the second site whereby its affinity increases. We believe this to be very unlikely in view of the rigid structure of the leucine zipper dimer. This kind of positive cooperativity between preexisting binding sites would seem to require a larger and conformationally more adaptable structure. We therefore propose a model in which the two GCN4-bound scFv fragments interact with each other. scFv fragments are known to dimerize and oligomerize (*35*, *38*, *39*). Although free scFv SW1 in the micromolar concentration range was monomeric, two scFv molecules suitably oriented on GCN4 could interact with each other and thereby stabilize the ternary complex $(scFv)_2$−GCN4. In other words, we hypothesize that the observed high cooperativity does not originate from cooperative antigen−antibody interaction but from accidental interaction of two adjacent scFv fragments bound to GCN4.

Energetics of scFv Binding. The thermodynamic parameters do not pertain to individual binding sites but average over the two GCN4-bound scFv fragments. Enthalpy-driven association seen here seems common to antigen−antibody association (*46*, *47*). The mean heat capacity change was moderate and negative, indicating that a considerable amount of hydrophobic surface was buried upon binding. The value is in the range of the results obtained with monoclonal antibodies and their antigens (*20*, *47*). The change with temperature of the partial specific heat capacity measured in DSC was larger than for most well-packed protein domains undergoing a cooperative two-state transition (*48*, *49*). However, little is known on the thermodynamic stability of scFv fragments and no other data on partial specific heat capacity changes over an extended temperature range are known to us. Interdomain vibrational modes are expected to be significant for a two-domain protein like a scFv fragment (*50*) and could increase the slope of the observed C_p/T trace.

Kinetics of scFv Binding. The association reaction was very fast and could be described by a simple one-step mechanism. The on rate constant of 1×10^6 M^{-1} s^{-1} is only about 100 times less than the diffusion limit estimated at 10^8 M^{-1} s^{-1} for the reaction of a monoclonal antibody with a small protein (*51*). Binding of two scFv fragments should, in principle, lead to two kinetic phases unless the two binding sites are independent. However, the two phases could not be resolved because the time resolution of the stopped-flow instrument was insufficient and also because the amount of scFv−GCN4 formed was small. In the simplest case, k_{on} calculated according to eq 2 is half the binding rate constant for the first scFv fragment.[4]

Dissociation could only be observed in the biosensor experiment and was very slow and incomplete. This behavior was observed in other antigen−antibody systems (*34*, *52*). The reasons are unclear. One possibility is that rebinding of the scFv fragment slowed the rate of dissociation and may have prevented complete dissociation during the observation interval. However, inclusion of excess free $GCN4_{SS}$ in the dissociation buffer did not increase the rate of dissociation and did not produce baseline regeneration (not shown). Hence, rebinding hardly affected the dissociation rate. Another possibility was that some scFv fragments were "sterically trapped" in the surface matrix of the sensor chip and were not freely accessible to buffer.

Significantly slower association to the surface-bound antigen in the biosensor experiment could have different reasons. Steric effects at the solid/liquid interface may lead to a heterogeneous antigen population. Also, the cooperativity could have been less strong on the surface-bound GCN4 dimer, again for reasons of steric accessibility. Less than perfect fits to a simple one-step binding reaction have been observed previously in BIAcore and other biosensor measurements with whole antibodies (*44*, *53*, *54*) and also with scFv fragments (*52*, *55*) and were interpreted by mass transport and surface heterogeneity effects.

In conclusion, this work exemplifies a very fast reaction of a scFv fragment with the leucine zipper motif. The reaction was enthalpy-driven and opposed by a negative entropy change. Two scFv fragments bound to a single rod-shaped leucine zipper, and binding was highly cooperative. This is tentatively explained by fortuitous interaction of two scFv fragments on the antigen. We are not aware of another example of cooperative antibody binding to a single protein molecule and are now attempting to solve the structure of $(scFv)_2$−GCN4. The discrepancies between the kinetics measured by stopped-flow and by biosensor call for a cautious interpretation of absolute kinetic parameters obtained

in solution and in a biosensor at a solid/liquid interface.

ACKNOWLEDGMENT

We thank Drs Antonio Baici, Peter Gehrig, and Stefan Klauser for assistance. A valuable suggestion by an anonymous referee is appreciated.

REFERENCES

1. Padlan, E. A. (1994) *Mol. Immunol. 31,* 169−217.
2. Winter, G., and Milstein, C. (1991) *Nature 349,* 293−299.
3. Clauss, M. A., and Jain, R. K. (1990) *Cancer Res. 50,* 3487−3492.
4. Raag, R., and Whitlow, M. (1995) *FASEB J. 9,* 73−80.
5. Owens, R. J., and Young, R. J. (1994) *J. Immunol. Methods 168,* 149−165.
6. Better, M., Chang, C. P., Robinson, R. R., and Horwitz, A. H. (1988) *Science 240,* 1041−1043.
7. Skerra, A., and Plückthun, A. (1988) *Science 240,* 1038−1041.
8. Huston, J. S., Levinson, D., Mudgett-Hunter, M., Tai, M. S., Novotny, J., Margolies, M. N., Ridge, R. J., Bruccoleri, R. E., Haber, E., Crea, R., et al. (1988) *Proc. Natl. Acad. Sci. U.S.A. 85,* 5879−5883.
9. Bird, R. E., Hardman, K. D., Jacobson, J. W., Johnson, S., Kaufman, B. M., Lee, S. M., Lee, T., Pope, S. H., Riordan, G. S., and Whitlow, M. (1988) *Science 242,* 423−426.
10. Glockshuber, R., Malia, M., Pfitzinger, I., and Plückthun, A. (1990) *Biochemistry 29,* 1362−1367.
11. Burton, D. R., and Barbas, C. F. I. (1994) *Adv. Immunol. 57,* 191−280.
12. Winter, G., Griffiths, A. D., Hawkins, R. E., and Hoogenboom, H. R. (1994) *Annu. Rev. Immunol. 12,* 433−455.
13. Richardson, J. H., and Marasco, W. A. (1995) *Trends Biotechnol. 13,* 306−310.
14. Marasco, W. A. (1995) *Immunotechnology 1,* 1−19.
15. Hinnebusch, A. G. (1984) *Proc. Natl. Acad. Sci. U.S.A. 81,* 6442−6446.
16. Hope, I. A., and Struhl, K. (1985) *Cell 43,* 177−188.
17. Hill, D. E., Hope, I. A., Macke, J. P., and Struhl, K. (1986) *Science 234,* 451−457.
18. Hai, T. W., Liu, F., Coukos, W. J., and Green, M. R. (1989) *Genes Dev. 3,* 2083−2090.
19. Dwarki, V. J., Montminy, M., and Verma, I. M. (1990) *EMBO J. 9,* 225−232.
20. Leder, L., Berger, C., Bornhauser, S., Wendt, H., Ackermann, F., Jelesarov, I., and Bosshard, H. R. (1995) *Biochemistry 34,* 16509−16518.
21. Wendt, H., Berger, C., Baici, A., Thomas, R. M., and Bosshard, H. R. (1995) *Biochemistry 34,* 4097−4107.
22. Berger, C., Jelesarov, I., and Bosshard, H. R. (1996) *Biochemistry 35,* 14984−14991.
23. Berger, C., Piubelli, L., Haditsch, U., and Bosshard, H. R. (1998) *FEBS Lett. 425,* 14−18.
24. Gill, S. C., and von Hippel, P. (1989) *Anal. Biochem. 182,* 319−326.
25. Krebber, A., Bornhauser, S., Burmester, J., Honegger, A., Willuda, J., Bosshard, H. R., and Plückthun, A. (1997) *J. Immunol. Methods 201,* 35−55.
26. Schier, R., Bye, J., Apell, G., McCall, A., Adams, G. P., Malmqvist, M., Weiner, L. M., and Marks, J. D. (1996) *J. Mol. Biol. 255,* 28−43.
27. Ge, L., Knappik, A., Pack, P., Freund, C., and Plückthun, A. (1995) in *Expressing antibodies in Escherichia coli* (Borrebaeck, C. A. K., Ed.) pp 229−266, University Press, Oxford, U.K.
28. Buchner, J., Pastan, I., and Brinkmann, U. (1992) *Anal. Biochem. 205,* 263−270.
29. Lindner, P., Bauer, K., Krebber, A., Nieba, L., Kremmer, E., Krebber, C., Honegger, A., Klinger, B., Mocikat, R., and Plückthun, A. (1997) *BioTechniques 22,* 140−149.
30. Wiseman, T., Williston, S., Brandts, J. F., and Lin, L.-N. (1989) *Anal. Biochem. 179,* 131−137.
31. Jelesarov, I., Leder, L., and Bosshard, H. R. (1996) *Methods: A Companion to Methods Enzymol. 9,* 533−541.
32. Plotnikov, V. V., Brandts, J. M., Lin, L. N., and Brandts, J. F. (1997) *Anal. Biochem. 250,* 237−244.
33. Wendt, H., Leder, L., Härmä, H., Jelesarov, I., Baici, A., and Bosshard, H. R. (1997) *Biochemistry 36,* 204−213.
34. Bernard, A., and Bosshard, H. R. (1995) *Eur. J. Biochem. 230,* 416−423.
35. Desplancq, D., King, D. J., Lawson, A. D., and Mountain, A. (1994) *Protein Eng. 7,* 1027−1033.
36. Ellenberger, T. E., Brandl, C. J., Struhl, K., and Harrison, S. C. (1992) *Cell 71,* 1223−1237.
37. König, P., and Richmond, T. J. (1993) *J. Mol. Biol. 233,* 139−154.
38. Whitlow, M., Filpula, D., Rollence, M. L., Feng, S. L., and Wood, J. F. (1994) *Protein Eng. 7,* 1017−1026.
39. Kortt, A. A., Lah, M., Oddie, G. W., Gruen, C. L., Burns, J. E., Pearce, L. A., Atwell, J. L., McCoy, A. J., Howlett, G. J., Metzger, D. W., Webster, R. G., and Hudson, P. J. (1997) *Protein Eng. 10,* 423−433.
40. Jelesarov, I., and Bosshard, H. R. (1994) *Biochemistry 33,* 13321−13328.
41. Krylov, D., Olive, M., and Vinson, C. (1995) *EMBO J. 14,* 5329−5337.
42. Zitzewitz, J. A., Bilsel, O., Luo, J. B., Jones, B. E., and Matthews, C. R. (1995) *Biochemistry 34,* 12812−12819.
43. Ramsden, J. J. (1997) *J. Mol. Recognit. 10,* 109−120.
44. Glaser, R. W. (1993) *Anal. Biochem. 213,* 152−161.
45. Altschuh, D., Dubs, M.-C., Weiss, E., Zeder-Lutz, G., and Van Regenmortel, M. H. V. (1992) *Biochemistry 31,* 6298−6304.
46. Tello, D., Goldbaum, F. A., Mariuzza, R. A., Ysern, X., Schwarz, F. P., and Poljak, R. J. (1993) *Biochem. Soc. Trans. 21,* 943−946.
47. Schwarz, F. P., Tello, D., Goldbaum, F. A., Mariuzza, R. A., and Poljak, R. J. (1995) *Eur. J. Biochem. 228,* 388−394.
48. Makhatadze, G. I., Medvedkin, V. N., and Privalov, P. L. (1990) *Biopolymers 30,* 1001−1010.
49. Privalov, P. L., and Makhatadze, G. I. (1992) *J. Mol. Biol. 224,* 715−723.
50. Tidor, B., and Karplus, M. (1994) *J. Mol. Biol. 238,* 405−414.
51. Raman, C. S., Jemmerson, R., Nall, B. T., and Allen, M. J. (1992) *Biochemistry 31,* 10370−10379.
52. Nieba, L., Krebber, A., and Plückthun, A. (1996) *Anal. Biochem. 234,* 155−165.
53. O'Shannessy, D. J. (1994) *Curr. Opin. Biotechnol. 5,* 65−71.
54. Oddie, G. W., Gruen, L. C., Odgers, G. A., King, L. G., and Kortt, A. A. (1997) *Anal. Biochem. 244,* 301−311.
55. Dougan, D. A., Malby, R. L., Gruen, L. C., Kortt, A. A., and Hudson, P. J. (1998) *Protein Eng. 11,* 65−74.
56. Weiss, M. A. (1990) *Biochemistry 29,* 8020−8024.
57. Bernasconi, C. F. (1976) *Relaxation Kinetics*, Academic Press, New York.

BI980874M